Process Biochemistry
November 2018, Volume 74, Pages 175-184
http://dx.doi.org/10.1016/j.procbio.2018.06.021
http://archimer.ifremer.fr/doc/00445/55694/

Concentration and purification of *Porphyridium cruentum* exopolysaccharides by membrane filtration at various cross-flow velocities

Balti Rafik [1, 2], Le Balc'h Romain [1], Brodu Nicolas [1, 3], Gilbert Marthe [1], Le Gouic Benjamin [1], Le Gall Sophie [4], Sinquin Corinne [5], Masse Anthony [1, *]

[1] LUNAM, Université de Nantes, GEPEA, UMR-CNRS 6144, 37 Bd Université, 44602 Saint-Nazaire, France
[2] Unité de Physiologie Fonctionnelle et Valorisation des Bio-Ressources (PFVBR), Higher Institute of Biotechnology of Beja, University of Jendouba, PB 382, Habib Bourguiba Avenue, 9000 Beja, Tunisia
[3] Normandie Univ, UNIROUEN, INSA Rouen, LSPC, 76000 Rouen, France
[4] INRA UR1268 Biopolymers Interactions & Assemblies (BIA), Rue de la Geraudière, 44300 Nantes, France
[5] IFREMER, EM3B Laboratory, Rue de l'Ile d'Yeu, 44311 Nantes Cedex 3, France

* Corresponding author : Rafik Balti, email address : anthony.masse@univ-nantes.fr

Abstract :

Exopolysaccharides (EPS) from cell-free *Porphyridium cruentum* media were concentrated then purified (diafiltration) on a 0.14 µm ceramic membrane. The influence of cross-flow velocities on filtration performances was investigated. Mean permeate fluxes equal to 49.8, 68.9 and 81.9 L.h-1. m-2 were obtained during the concentration at 4 bar for respectively cross-flow velocities inside the membrane lumen equal to 2.5, 3.3 and 4.2 m.s-1; 49.7 L.h-1. m-2 for the diafiltration at 3.3 m.s-1. Permeate fluxes were correctly predicted from polysaccharide concentrations (10 % deviation). Volume reduction factors higher than 7.8 were reached. Rejection rates of polysaccharides and proteins varied according to the cross-flow velocities. Thus, the EPS recovery rate or time of filtration could be modulated following the cross-flow velocity. Polysaccharides were concentrated 6.3 to 10.4 times in such a way that the final sugars concentration reached 1.74 to 2.26 g.L-1. Rheological behavior of filtered solutions changed following the concentration progress. More than 80 % (w/w) of polysaccharides were recovered while 49 % and 99 % of proteins and salts were removed respectively. The filtrations allowed reaching a final monosaccharide content of dry matter equal to 48.9 % against 0.6 % (w/w) initially.

Graphical abstract

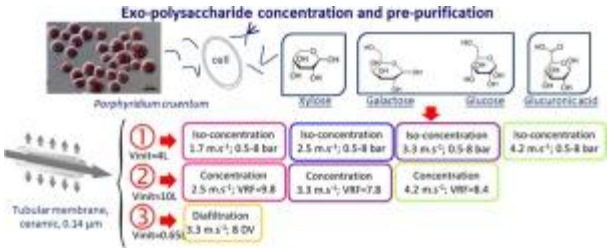

Highlights

► Simple and rapid micro-alga's exopolysaccharide (EPS) concentration and purification ► High yields of EPS recovery and good permeate fluxes ► Change of rheological behaviour and composition of filtered solutions during filtration ► Time and degree of concentration change following the cross-flow velocity ► Advanced characterization of extracts

Keywords : Membrane filtration ; exopolysaccharides ; microalga ; concentration ; diafiltration

1. Introduction

Currently, there is an increasing market demand for natural polysaccharides for the food, cosmetics and pharmaceutical industries. In particular, microalga polysaccharides receive much attention. Those coming from *Porphyridium* have important techno-functional and biological properties [1]. Thus, their recovery should be part of a strategy of complete bio-refinery of the microalga culture.

Porphyridium cruentum is a eukaryotic red marine microalga (Rhodophyta) which has a relatively fast growth rate and the possibility to regulate its growth [2]. Various carbohydrates can be found as (i) storage polymers (starch floridea), (ii) lipopolysaccharides of the cell wall and (iii) extra- or exo-cellular polysaccharides (EPS). The last one can be bounded to the cell (capsular polysaccharides) or loosely linked to the cell (slime) and even

released/dissolved into the growth medium. The capsular polysaccharides constitute a protection for the micro-algae against desiccation, predators or any environmental changes such as pH, temperature, salinity, irradiance, etc. [3, 4]. The soluble EPS are naturally synthesized and secreted by membrane-mediated exocytosis or after a physiological stress [5]. The amounts of soluble EPS change according to the physiological state of microalgae and culture conditions as well as strain, culture media, mode of cultivation (batch, continuous), illumination, salinity, etc. [5]. The concentrations of soluble exopolysaccharides of *Porphyridium*

(0.1-0.7 $g.L^{-1}$) are in the range of relatively high producing microalgae such as *Arthrospira platensis* (0.37 $g.L^{-1}$), *Rhodella violacea* (0.2-0.6 $g.L^{-1}$), *Botryococcus braunii* (0.25-1 $g.L^{-1}$) and *Dunaliella salina* (0.94 $g.L^{-1}$) [6, 3, 7, 8, 9, 10, 11, 12]. The exopolysaccharides of *Porphyridium* are often formed by polymerizing a large number (more than 10) of various monosaccharides (heteropolysaccharides) such as pentoses and hexoses. Monosaccharides are poly-alcohols (OH) comprising a carbonyl (aldehyde (-CHO) or ketone (-C=O)) and sometimes amine ($-NH_2$) or carboxylic (-COOH) function. They may be connected by O-glycosidic linkages. Consequently, exopolysaccharides can exhibit an acidic character in alkaline medium.

Currently, the soluble or solubilized exopolysaccharides are classically separated from cells by centrifugation or microfiltration [5, 13, 14]. Bounded EPS can be solubilized by addition of formaldehyde, ethylene diamine tetracetic acid and sodium hydroxide or by sonication, heating, complexation and ion exchange [1, 15]. Then, soluble or solubilized exopolysaccharides are traditionally extracted and purified using dialysis against distilled water or precipitation with alcohols (methanol, ethanol and isopropanol) or cationic surfactants [5, 16, 17]. These techniques can lead to the extraction of low-purity polymers with high salt content and poor solubility, incompatible with industrial application [18]. In

fact, *Porphyridium* is often cultivated into artificial seawater which complicates the exopolysaccharides purification [19]. Finally, the extraction/purification procedures are often environmentally unfriendly and are designed for laboratory scale that means for analytical purposes.

Few studies suggest using tangential ultra- or microfiltration to concentrate, desalt and pre-purify soluble EPS whereas high degree of purity can be obtained [18, 20, 21]. Ultrafiltration is already used for natural sensitive compounds because no chemical addition is needed and the operating conditions (temperature, shear stress, pressure) are relatively soft. The membrane filtration is notably useful for the concentration of large volumes. It is a mature technology which finds applications at industrial scale. Nevertheless, the membrane fouling is often a key issue to be resolved, notably for the filtration of solutions with high EPS concentrations. In fact, the negatively charged carboxylated and sulfated exopolysaccharides produced by micro-alga, exhibit high stickiness and propensity to form slimy gels which could severely foul the membranes [22]. Moreover, the EPS solutions are highly viscous even at low concentrations. So, the operating conditions of the membrane filtration, notably hydrodynamic conditions inside the membrane lumen should influence the fouling intensity. Consequently, it was chosen to study the effect of the cross-flow velocity on the filtration performances. The aim of this study was also to set-up a simple refining chain (limited number of steps) capable of concentrating and purifying the EPS solutions without the addition of chemicals.

2. Material and methods

2.1. Microalga cultivation, harvesting and conditioning

The *P. cruentum* microalga (UTEX 161) was grown in batch mode within a tubular photo-bioreactor (110 L) at 25 °C (+/- 2 °C) inoculated from a prior culture in an Airlift PBR (10 L).

A modified Bold's basal medium was used for the cultivation. The pH was regulated at 7.5 and the incident photon flux was equal to 120 µmol.m^{-2}.s^{-1}. Directly after harvesting, the culture was stored for 24 hours in darkness, at ambient temperature (approximately 20 °C), to release a part of the bounded EPS. No bubbling of CO_2 or air was carried out during the storage. Then, microalga cells were separated from the culture medium by centrifugation (Thermo Scientific Sorvall RC6 Plus, Thermo Fisher, France) at 17600 g during 25 minutes at 4 °C. Firstly, the supernatant (often referred to cell-free medium or feedstock in this article), which contains the EPS, was stored at -20 °C before thawing at ambient temperature for at least 12 hours, just before the membrane filtration experiments.

2.2. Microfiltration experiments

2.2.1. Description of the microfiltration set-up

Membrane microfiltration was performed on a pilot-scale set-up equipped with a 0.032 m² tubular ceramic membrane (TAMI Industries, Inside CeRAM, Cell 60, 7 channels) having a mean pore diameter and water permeability equal to 0.14 µm and 75 ± 6.1 L.h^{-1}.m^{-2}.bar^{-1}, respectively [23]. All filtrations were carried out at 20 °C, in batch mode. The trans-membrane pressure (TMP) was kept constant during experiments. After each experiment and following manufacturer recommendations, the membrane was cleaned with sodium hydroxide solution (pH = 12) at 60 °C for 30 minutes in closed loop (recirculation of permeate and retentate into the feed tank). Then, the pilot plant was flushed by milliQ water until neutral pH at 20 °C in open loop (discharge of the permeate). Afterward, the membrane was cleaned using a nitric acid solution (pH = 1.2) at 50 °C for 15 minutes in closed loop. Finally, the membrane was flushed by milliQ water until neutral pH. This procedure was also used for membrane deconditioning. More than 90 % of the water fluxes were recovered after the cleaning.

2.2.2. Operating conditions for the iso-concentration mode

The crude cell-free medium obtained after centrifugation (Thermo Scientific Sorvall RC6 Plus, Thermo Fisher, France) at 1700 g during 25 minutes at 4 °C was filtered. Iso-concentration filtrations were carried out that means filtrations with retentate and permeate re-circulation to the feed tank. Various cross-flow velocities (1.7, 2.5, 3.3, 4.2 $m.s^{-1}$) and trans-membrane pressure (0.5 to 8 bar) were investigated. The Reynolds number at the entrance of the membrane channels was equal to 3321, 4981, 6641, 8301 and the wall shear stresses were equal 25, 31, 48 and 68 Pa for cross-flow velocities respectively equal to 1.7, 2.5, 3.3 and 4.2 $m.s^{-1}$. Microfiltration is classically carried out in this range of cross-flow velocities in order to be in a turbulent regime as shown by the Reynolds number (above about 3000). Thus, in most cases, the membrane fouling could be mitigated comparatively to laminar regime. Nevertheless, it should be noted that during the concentration step, the density and viscosity of the crude cell-free medium will change which will reduce the Reynolds number. Thus, the conditions could pass from a turbulent regime to a laminar one. For each TMP, the permeate flow was measured every 10 minutes until permeate flux stabilization.

2.2.3. Operating conditions and modeling of the concentration stage

Batch mode was used to concentrate the crude cell-free medium at 4 bar, until a Volume Reduction Factor (VRF) equal to 7-10 is reached. The concentration process was carried out at 2.5, 3.3 and 4.2 $m.s^{-1}$. The mean retention rate (R) of sugars was calculated for each concentration experiment. It is linked to the initial retentate concentration ($C_{R0.Sugar}$) and over time ($C_{R.Sugar}$) as well as the volume reduction factor (VRF) as mentioned in the Cheryan's book [24]:

$$C_{R.Sugar} = C_{R0.Sugar} \times VRF^{R} \qquad \text{equation 1}$$

The evolution of permeate flux (J) was modeled in function of the retentate concentration ($C_{R.Sugar}$) (Appendice A):

$$J = k \,.\, \ln (C_{gel} / C_{R.Sugar}) \qquad \text{equation 2}$$

A mean mass transfer coefficient (k) was considered during the concentration step. The sugar concentrations of permeates were assumed negligible compared to retentates. Gel concentration (C_{gel}) can be empirically evaluated from the curve giving the permeate fluxes versus the logarithms of the sugar concentrations of retentates. Moreover, the mass transfer coefficient (k) was related to the cross-flow velocity at the membrane surface as:

$$k = B \,.\, u^{n} \qquad \text{equation 3}$$

B and n are constants determined experimentally. On the other hand, ones try to estimate the permeate fluxes by a power law, function of the sugar concentration of the retentate and the cross-flow velocity:

$$J = \beta \, C_{R.Sugar}^{a} \,.\, u^{b} \qquad \text{equation 4}$$

For the present work, the mean absolute percentage error (MAPE) was calculated for both models (equation 2 and 4) in order to evaluate the prediction accuracy:

$$MAPE = 1/n \,.\, \Sigma[|(J_{model} - J_{exp})| / J_{exp}] \qquad \text{equation 5}$$

Where, n is the number of experimental points while (J_{model}) and (J_{exp}) are the predicted and experimental permeate fluxes, respectively.

2.2.4. Operating conditions and modeling of the diafiltration stage

During the diafiltration at 4 bar and 20 °C, MilliQ water was added (pH and conductivity respectively equal to 6.5 and 0.12 $mS.cm^{-1}$) in order to keep constant the volume of liquid (650 mL) into the feed tank. The same cross-flow velocity was chosen for the concentration

and diafiltration steps (3.3 $m.s^{-1}$). No samples of retentate were taken during the diafiltration due the low initial volume inside the feed tank; to take samples would change a lot the volume within the feed tank. The solute concentration within the feed tank (C'_R or C'_{R0} for the initial solute concentration) is linked to the retention rate (R') and the number of diavolume (DV) as mentioned in the Cheryan's book [24]:

$$C'_R = C'_{R0} \cdot e^{(R'-1)\,DV} \qquad \text{equation 6}$$

The number of diavolume is defined as the ratio of the volume of water added to the feed tank (V_W) and the initial feed tank volume (V_0).

2.3. Biochemical analysis

2.3.1. Total sugar analysis

EPS content was evaluated by colorimetric method after adding phenol and sulfuric acid as described by Dubois *et al*. [25]. In the presence of sulfuric acid, sugars are hydrolyzed, dehydrated and rearranged to form furfural. By condensation with phenol, the compounds lead to a yellow coloration. Typically, 500 µL of sample was introduced at the bottom of a 15 mL polypropylene falcon tube. Then, 500 µL of phenol solution (50 $g.L^{-1}$) was added to 2.5 mL of sulfuric acid (> 96%). After 10 minutes of incubation at ambient temperature, each tube was homogenized for 10 seconds (vortex at 3000 rpm). The tubes were incubated for 15 minutes at ambient temperature and then for 30 minutes at 35 °C. Finally, the absorbance at 483 nm was measured using a spectrophotometer (Jasco V630, Bouguenais, France). Each sample was analyzed in triplicate. The calibration curve was made using D-glucose.

2.3.2. Soluble protein determination

Protein content was determined by Lowry's method, using a Sigma-Aldrich kit (BCA1-1KT) [26]. Basically, in alkaline conditions, proteins react with copper to form a cupric complex which is then reduced in cuprous ions, giving a purple color to the solution. First, a solution

was prepared by adding 50 mL of BCA solution (Sigma-Aldrich, B9643, bicinchoninic acid, sodium tartrate and sodium bicarbonate in NaOH at 0.1 N, pH = 11.25) and 1 mL of copper sulfate (Sigma-Aldrich, C2284, $CuSO_4.5H_2O$, 40 $g.L^{-1}$). Then, 100 µL of the sample was added to 2 mL of test solution in a 15 mL polypropylene falcon tube. The blank was made with milliQ water. The tubes were homogenized for 5 seconds (vortex at 3000 rpm) before being incubated at 37 °C for 30 minutes. The calibration curve was carried out using Bovine Serum Albumin (BSA) (Sigma-Aldrich, P0914). Finally, the absorbance at 562 nm was measured using V-630 spectrophotometer (Jasco, Bouguenais, France). Each sample was analyzed in triplicate.

2.3.3. Dry matter and ash content determination

Cell-free medium and retentates were freeze-dried (Christ Alpha 1-2 LD Plus, France) then placed in pre-weighed crucible and dried at 105 °C then 550 °C until constant mass. Thus, the dry matter and ash were determined respectively. The values presented are the average of three measurements.

2.3.4 Molecular weight determination

The molecular weight was determined by high-performance size-exclusion chromatography (HPSEC) coupled on line with a multiangle light scattering detector (MALS, Dawn Heleos-II, Wyatt Technology Sc , Toulouse, France) and a differential refractive index detector (Optilab, Wyatt Technology Sc, Toulouse, France). HPSEC system was composed of an HPLC system (Prominence Shimadzu, Marne la Vallée, France) a PL aquagel-OH mixed, 8 μm (Agilent Technologies France S.A.S, Massy, France) guard column (50 x 7.5 mm) and a PL aquagel-OH mixed (Agilent Technologies France S.A.S, Massy, France) separation column (300 x 7.5 mm). Elution was performed at 1 $mL.min^{-1}$ with 0.1 M ammonium acetate containing 0.03 % NaN_3. Injected samples contained 2 or 10 milligrams of dry matter per milliliter; 100 µL were

injected. Data were computed with Astra 6.1 software (Wyatt Technology Sc, Toulouse, France) fusing a specific refractive index increment (d*n*/d*c*) value of 0.145 $mL.g^{-1}$.

2.3.5. Monosaccharide analysis

Identification and quantification of neutral sugars were performed by gas-liquid chromatography (GC) after sulfuric acid degradation [27]. Five milligrams of dry matter were hydrolyzed in 1 M sulfuric acid (2 h, 100 °C). Sugars were converted to alditol acetates according to Blakeney *et al.* [28] and chromatographed on a TG-225 GC Column (30 x 0.32 mm ID) using TRACE™ Ultra Gas Chromatograph (Thermo Scientific™; temperature 205 °C, carrier gas H_2). Standard sugar solution and inositol as internal standard were used for calibration. Standards refer to L-Rhamnose monohydrate (Sigma Aldrich, 83650), L-(−)-Fucose (Sigma Aldrich, F2252), L-(+)-Arabinose (Sigma Aldrich, A3256), D-(+)-Xylose (Sigma Aldrich, X3877), D-(+)-Mannose (Sigma Aldrich, M2069), D-(+)-Galactose (Sigma Aldrich, G0750), D-(+)-Glucose (Sigma Aldrich, G8270) and myo-Inositol (Sigma Aldrich, I5125). Uronic acids in acid hydrolyzates were quantified using the metahydroxydiphenyl colorimetric acid method [29].

2.3.6. Rheology analysis

The viscosity was measured using an Anton paar MCR 500 rheometer (Anton Paar, Courtaboeuf, France). Measurements were carried out at 20 °C using a coaxial roller system (DG 26.7) with a shear rate ranged from 15 to 1000 s^{-1}. A sample of 3.6 mL was required for each assay. The rheological behavior of the non-newtonian fluid was described by a power law:

$$\eta = K \cdot \dot{\gamma}^{n-1} \qquad \text{equation 7}$$

η is the viscosity value corresponding to the shear rate $\dot{\gamma}$ while K and n are respectively the consistency and the behavior index.

2.3.7. Total Carbon and Total Nitrogen measurements

Total Carbon and Total Nitrogen were determined with an automated dry combustion method (Dumas method) using an elemental analyser (vario MICRO cube, Elementar Analysensysteme, Hanau, Germany).

3. Results and discussion

3.1. Biochemical characterization of the crude cell-free medium

The pH and conductivity of the initial cell-free medium are respectively equal to 8 and 22.0 $mS.cm^{-1}$. The volume mass and dynamic viscosity at 20 °C are equal to 998.16 $kg.m^{-3}$ and 1.004×10^{-3} Pa.s. A large part of the dry matter weight (92.7 %) is mineral and probably comes from the salts of the modified Bold's basal medium (Table 1). The carbon, nitrogen and sulfur represent respectively 0.77, 1.96 and 0.16 % of the dry matter weight. The sulfates could come from sulfated exopolysaccharides [30]. Indeed, Ramus [5] or Arad *et al.* [2] found 7-8 % by weight of sulfate into the dissolved exopolysaccharides of *Porphyridium*. On the basis of the nitrogen results, the dry matter of the crude medium would be composed of 4.9 % (w/w) of proteins [31]. These proteins (1-2 %) could be linked to the polysaccharides [2, 32]. The average of soluble protein and sugar concentrations are equal to 0.03 and 0.26 $g.L^{-1}$ (Table 1). Exopolysaccharides contain xylose, galactose, glucose and glucuronic acid in the molar ratios of 1.5/1.3/0.6/0.5. Thus, as already found, *Porphyridium* EPS are mainly composed of neutral monosaccharides [7, 33, 34, 35]. Additional minor carbohydrates such as mannose, rhamnose, arabinose, ribose, uronic acids and methylated carbohydrates are sometimes found [18, 36, 37, 38, 39, 40]. The weight-average molar mass and gyration radius of this polymer are equal to 2.4×10^6 Da and 173 nm, respectively (Table 2). This result confirms that the molar mass of *Porphyridium* EPS is ranged between 2 and 7×10^6 Da [34, 37, 39]. The polydispersity index, 1.18, is low as some other microbial exopolysaccharides from probiotic *Lactobacillus plantarum* (1.05) and from an enthomopathogenic fungus *Cordyceps militaris* (1.00 to 1.18) [41, 42].

3.2. Selection of the working pressure for subsequent concentration stages

The values of the pseudo-stabilized permeation fluxes for various trans-membrane pressures and cross-flow velocities are shown on Figure 1. As classically found, the pressure-controlled region takes place at low trans-membrane pressures where increasing the trans-membrane pressure increases linearly the permeate flux. The permeate fluxes become almost constant from approximately 4 bar. The highest permeate flux (168 $L.h^{-1}.m^{-2}$) was reached at 4.2 $m.s^{-1}$ and 8 bar.

During these iso-concentration experiments, the crude cell-free medium would have an almost Newtonian behaviour. Thus, the change of cross-flow velocities will induce a change of shear stress at the membrane surface without change of cell-free medium viscosity. Therefore, the change of permeate flux values from one cross-flow velocity to another would not be induced by a change of viscosity. On the basis of these first results (Figure 1), it was chosen to operate at 4 bar for the subsequent concentration and diafiltration experiments. For the most part of cross-flow velocities, TMP higher than 4 bar will not induce a much faster operation since the limiting flux is almost reached. With lower TMP, the permeate fluxes will be reduced which will affect the production capability of operation.

3.3. Study of the concentration step of the crude cell-free medium.

3.3.1. Evaluation of the permeate fluxes and selectivity

As a result of the concentrations, the volume of the crude cell-free medium is reduced between 7.8 to 9.8 folds (Figure 2.a). It takes between 3 and 6 h to concentrate 7 to 10 L of EPS solution. The permeate fluxes obtained in the early phases of the filtration are the lowest for the concentration at 2.5 $m.s^{-1}$ and substantially highest for the experiments at 3.3 and 4.2 $m.s^{-1}$. At the end of the concentration process, the permeate fluxes are equal to 30-50 $L.h^{-1}.m^{-2}$. The permeate fluxes drop with the onset of the filtration. Thus, no limit concentration exists from which the permeate flux would begin to fall as already seen during the ultrafiltration of

microbial exopolysaccharide (xanthan) [43]. In contrast, as found by Shu-Sen [44], the infinite increase of viscosity at the beginning of the concentration process could contribute to the high decrease of permeate flux. Thus, permeate fluxes would decrease due to the fouling of the membrane, the polarization concentration and changes of fluid characteristics being filtered. The hydrodynamic conditions change according to the chosen cross-flow velocity but also during the concentration process due to an increase of the viscosity (Figure 3). For instance, the rheological study carried out on concentrates of the experiment at 3.3 $m.s^{-1}$ shows that the viscosity obtained for a shear rate of 15 s^{-1}, passes from 4.6 to 18.7 mPa.s while the sugar concentrations increase from 0.48 to 1.74 $g.L^{-1}$. The values of viscosity are in the same order of magnitude, if not slightly lower, than those found by Patel *et al.* [18]. The presence of salts could reduce the viscosity of solutions. In fact, the viscosity at 7.9 s^{-1} (25 °C) of a solution containing 0.1 % (w/v) of *Porphyridium* exopolysaccharides is reduced from 72.3 to 23.2 mPa.s in the presence of 0.1 M of NaCl [45]. Moreover, changes of rheological behaviour during the concentration process could be not only induced by a change of EPS or salt concentrations but also by a change of average EPS molecular weight [46]. Indeed, as will be seen later, the smallest EPS could pass through the membrane during the concentration process. As a consequence, the EPS population of the concentrates would change in the course of the concentration process. The value of the shear rate inside the membrane lumen is not known but if lower than 1000 s^{-1} the filtration could start with a Newtonian liquid of low viscosity, close to that of water, whereas from a certain value of sugar concentration the fluid would have a shear-thinning behavior. Indeed, the behavior index (n) of the power law applied between 15 and 1000 s^{-1} decreases from 0.731 to 0.464 during the concentration process. For reminder, the behavior index is equal to 1 for Newtonian fluid. Thus, rheological properties of *Porphyridium* EPS solutions seem comparable to xanthan's exopolysaccharides that's why

several data related to xanthan were used in this work in order to explain our results [35, 47, 48]. Nevertheless, several authors found a behavior index value close to 0.1 for *Porphyridium* exopolysaccharide solutions at around 0.1 % (w/v) which were prepared with distilled water [37, 43]. The composition of solutions (salts, impurities, etc.) could explain these differences of values since our results have been obtained directly on the concentrates and not on purified exopolysaccharides.

The EPS concentration passes from 0.26 $g.L^{-1}$ at the beginning to 1.74-2.26 $g.L^{-1}$ at the end of the concentration process according to the adopted cross-flow velocity (Figure 4). The amount of sugar within the final concentrates depends on the final volume reduction factor as well as the mean retention rate of each experiment. Thus, the highest final volume reduction factor (9.8) and mean sugar retention rate (97.5 % - obtained thanks to equation 1) of the 2.5 $m.s^{-1}$ experiment, lead to the highest sugar concentration (2.26 $g.L^{-1}$). The mean sugar retention rates of the experiments at 3.3 and 4.2 $m.s^{-1}$ are found to be equal to 90.3 and 80.3 %, respectively. Thus, in the case of the highest cross-flow velocities, sugars would pass more freely through the fouled membrane. Harscoat *et al.* [49] found the same trend during the microfiltration (ceramic membrane, 0.5 µm pore size, 100 kPa) of *Sinorhizobium meliloti* fermentation broth containing 1.4 to 1.6 $g.dm^{-3}$ of extracellular polysaccharides; sieving coefficient at 3 $m.s^{-1}$ was equal to 10 % versus 18 % at a cross-flow velocity of 6 $m.s^{-1}$.

The monosaccharide content (xylose, galactose, glucose and glucuronic acid) of the dry matter obtained at the end of each concentration experiment vary from 5.4 to 7.7 % (w/w) with the slightly highest content for the highest final volume reduction factor and retention rate that means 2.5 $m.s^{-1}$ experiment (Table 3). At the end of the concentrations, xylose, galactose, glucose and uronic acid represents, respectively and in average, 30.3, 31.5, 13.2 and 25.1 % (w/w) of total monosaccharides. A part of the exopolysaccharides could be sulphated because 0.16 (crude cell-free medium) to

0.32-0.39 % (final concentrates) of the dry matter weight contains sulphur (results not shown). The weight-average molar masses of EPS found in the final concentrates are ranged from 1.8 to 2.2 × 10^6 Da and don't vary so much between experiments (Table 2). Nevertheless, as already seen, molar masses could be slightly higher for the highest cross-flow velocities because of lower retention rates; in this case the smallest EPS could pass through the membrane [43].

The soluble protein concentrations into the final concentrates remain low between 0.15 and 0.18 $g.L^{-1}$, since only 59.9 to 63.9 % (w/w) are recovered (Table 1). Thus, the proteins are concentrated 5 to 6 folds against 6 to 10 for the exopolysaccharides. So, a pre-purification of exopolysaccharides begins during the concentration experiments. A part of the rest of proteins will be removed from the retentate during the subsequent diafiltration step. The chromatography technic could be used to pursue the purification.

The minerals (ash) to dry matter ratio (w/w) of the retentates decreases during the concentration stage from 92.7 % to 80.6-84.0 %. This result can be explained by the increase of the organic matter concentration such as sugars and proteins while salt concentration remains almost constant. The salt retention rate would be close to zero during the concentration step since ash content is quite stable. This partly explains why the pH and the conductivity remain almost constant during the concentration experiments. The pH of the raw solution to be filtered is equal to 8 against 8.2-8.3 at the end of the concentration steps; 22.0 and 22.0-25.1 $mS.cm^{-1}$ for the conductivity respectively. Once again, it should be noted that the concentration process allows eliminating salts, in addition to proteins, which induces the EPS purification.

3.3.2. Modeling and driving parameters of the concentration process

As a reminder, the evolution of permeate fluxes has been modelled in order to predict them in the case of future experiments. From the graphical representation of the permeate fluxes

versus the logarithm of sugar concentrations, an average mass transfer coefficient (k) and gel concentration (C_{gel}) are calculated (Appendice A). The gel polarization model is used in the area where membrane permeation rate is almost independent of the transmembrane pressure (Figure 1.b). On average the gel concentration is found to be equal to 5.4 $g.L^{-1}$; it varies between 5.07 and 5.68 $g.L^{-1}$, depending on the adopted cross-flow velocity. It should be noted that the increase of viscosity which occurs during the concentration process can either increase or decrease the mass transfer coefficient depending upon the flow regime [50]. Thus, what is determined here is an average mass transfer over the filtration time. This average mass transfer coefficient increases with the cross-flow velocity. It passes from 6.3×10^{-6} to 10.7×10^{-6} $m.s^{-1}$ when the cross-flow velocity is increased from 2.5 to 4.2 $m.s^{-1}$. The logarithm of the mass transfer coefficient (y-axis) is plotted in function of the logarithm of the cross-flow velocity (x-axis) in order to determine the coefficients B and n (Equation 3). Thus, for the present work the gel-polarization model can be written as:

$$J = 2.5x10^{-6} \cdot u^{1.02} \cdot \ln (5.4/C_{R.Sugar}) \qquad \text{equation 8}$$

Where J is the permeate flux ($m.s^{-1}$), u the cross-flow velocity ($m.s^{-1}$), ranged from 2.5 to 4.2 $m.s^{-1}$, and $C_{R.sugar}$ the sugar concentration of the retentate ($g.L^{-1}$).

On the other hand, the parameters of the power law described by the fourth equation, are found to be equal to 4.6×10^{-6}, -0.49 and 0.94 for respectively β, a, b. Thus, the model can be written as:

$$J = 4.6x10^{-6} \cdot C_{R.Sugar}^{-0.49} \cdot u^{0.94} \qquad \text{equation 9}$$

The permeate flux (J) is expressed in $m.s^{-1}$, the cross-flow velocity (u) in $m.s^{-1}$ and the sugar concentration of the retentate ($C_{R.sugar}$) in $g.L^{-1}$.

Permeate fluxes are slightly better predicted by the power law than by the gel-polarization model even if the mean absolute percentage errors remains relatively low

(Figure 2.b). Indeed, for both models, the mean absolute percentage errors (MAPE) on permeate flux prediction from the experimental sugar concentration is lower than 10 %. Thus, in the case of the gel-polarization model, the MAPE is equal to 7.9, 4.3, 4.5 % for respectively the concentration stage at 2.5, 3.3, 4.2 $m.s^{-1}$ against 7.7, 2.3 and 3.5 % for the power law model. In the case of the gel-polarization model, the prediction will probably be more accurate if the sugar permeate concentrations are not neglected against retentate ones and with a non-constant mass transfer coefficient during the concentration process. From the results of the modeling, the experimental points and for each cross-flow velocity, a graphic can be built in order to relate the time of filtration, the concentration factor (CF) and the volume reduction factor (Figure 5). It shows that the lowest cross-flow velocity (2.5 $m.s^{-1}$) allows having the highest final concentration factor (CF) even if the duration of the concentration will be high. Thus, with the experimental set-up used for this work, a maximum concentration factor (9.3 from the model and 10.4 experimentally) will be reached in the case of the experiment at 2.5 $m.s^{-1}$; it will take 320 minutes. By contrast, if a loss of sugar can be accepted during the concentration stage, highest cross-flow velocities could be taken in order to reduce the time of filtration. Thus, the cross-flow velocity is a key parameter which allows playing on sugar retention rate and consequently (i) on the time of filtration to reach targeted sugar concentration into the retentate or (ii) on the value of the final sugar concentration for a defined time of filtration.

3.4. Study of the desalting step by diafiltration

The diafiltration lasts 195 minutes which corresponds to an addition of 5.2 liters of MilliQ water that means a number of dia-volume equal to 8 (Table 1). The concentration followed by the diafiltration step allowed concentrating and pre-purifying the exopolysaccharides.

The permeate fluxes slightly increase in the course of the diafiltration from 40 to 59

$L.h^{-1}.m^{-2}$ (Figure 6). Thus, a part of compounds (smaller compounds) would be removed during the diafiltration process which induces a decrease of osmotic pressure as already suggested during the diafiltration of a clarified sugarcane juice on a PES spiral wound membrane (pore size of ~5 nm) [51]. The diafiltration could mitigate the polarization concentration phenomenon at the membrane surface and induces an increase of permeate fluxes. It should be noted that by considering only the influence of salts, the viscosity of the EPS solution could increase during the diafiltration. Indeed, Eteshola *et al.* [45] found that the viscosity of *Porphyridium* EPS solution (0.1 % (w/v)), obtained at 7.9 s^{-1}, is 3 folds higher without NaCl compared to a solution at 0.1 M NaCl. Salts would have a screening effect on charge-charge interactions along and between polysaccharide chains. Nevertheless, no increase of viscosity is visually observed during the present diafiltration; other compounds than salts could also act on solution viscosity.

The conductivity of solution that is being filtered decreases during the diafiltration from 25.1 to 0.2 $mS.cm^{-1}$ that means 99 % of reduction (Figure 6). A mean salt transmission rate equal to 62.5 % is found; the transmission rate is defined as the ratio of permeate on retentate conductivity and a linear relationship between conductivity and salt concentration was assumed. Thus, the conductivity of the retentate (in $mS.cm^{-1}$) is related to the number of diavolume (DV) as:

$$\text{Conductivity} = 22.14\ e^{-0.625\ DV} \qquad \text{equation 10}$$

About 18.5 % of proteins are lost during the diafiltration since it passes from 0.15 to 0.12 $g.L^{-1}$ (Table 1). Thus, organics, other than sugars, are removed during the diafiltration. No EPS is lost during the diafiltration that's why sugar concentration remains equal to 1.74 $g.L^{-1}$ into the desalted solution whereas, as previously seen, salts and proteins are partly removed (Table 1). At the end of the diafiltration, xylose, galactose, glucose and glucuronic acid represent respectively 31.7, 33.3, 13.7 and

21.2 % (w/w) of monosaccharides. Thus, monosaccharide content of the dry matter increases up to 48.9 % (w/w) after diafiltration (Table 3). In other words, the dry matter obtained after the full filtration chain contains 9.0 times (mass basis) more monosaccharides versus 125.5 times less salts. As expected, the diafiltration allows the purification of the EPS solution.

4. Conclusion

Porphyridium cruentum exopolysaccharides were concentrated more than 6 folds, and purified by ceramic membrane filtration. High yields of EPS recovery and good permeate fluxes were obtained. Final product was poorly salted, low in proteins but with nearly 2 $g.L^{-1}$ of exopolysaccharides. Thus, significant amounts of exopolysaccharides could be obtained in the case of important volumes of culture medium. EPS had molecular weight equal to 2.4×10^6 Da and contained xylose, galactose, glucose and glucuronic acids in the molar ratios of 1.5/1.3/0.6/0.5. On the basis of the results of this work, permeate fluxes obtained during the concentration or diafiltration steps could be estimated depending on exopolysaccharides concentration, the number of diavolumes or the volume reduction factors.

After completing the present work, it remains to study the influence of the filtration on the techno-functional properties of exopolysaccharides. Indeed, the properties and biological activities of EPS should not be lost in the course of membrane filtration.

Acknowledgments

A part of this study was carried out in the framework of Coselmar project supported by Ifremer and Nantes University and co-funded by the French Regional Council of the “Pays de la Loire”.

References

[1] C. Delattre, G. Pierre, C. Laroche, P. Michaud, Production, extraction and characterization of microalgal and cyanobacterial exopolysaccharides, Biotechnol. Adv. 34 (2016) 1159-1179.

[2] S.M. Arad, M. Adda, E. Cohen, The potential of production of sulfated polysaccharides from *Porphyridium,* Plant Soil. 89 (1985) 117-127.

[3] S.M. Arad, Production of sulfated polysaccharides from red unicellular algae, in : T. Stadler, J. Mollion, M.C. Verduset (Eds.), Algal Biotechnology-An Interdisciplinary Perspective, Elsevier Applied Science., London, UK, 1988; pp. 65-87.

[4] S.M. Arad, O.D. Friedman, A. Rotem, Effect of nitrogen on polysaccharide production in a *Porphyridium sp.,* Appl. Environ. Microbiol. 54 (1988) 2411-2414.

[5] J. Ramus, The production of extracellular polysaccharide by the unicellular red alga *Porphyridium aerugineum*, J. Phycol. 8 (1972) 97-111.

[6] M. Adda, J.C. Merchuk, S.M. Arad, Effect of nitrate on growth and production of cell-wall polysaccharide by the unicellular red alga *Porphyridium*, Biomass. 10 (1986) 131-140.

[7] S. Li, Y. Shabtai, S. M. Arad, Production and composition of the sulphated cell wall polysaccharide of *Porphyridium* (Rhodophyta) as affected by CO_2 concentration, Phycologia. 39 (2000) 332-336.

[8] Z. Csögör, B. Kiessling, I. Perner, P. Fleck, C. Posten, Growth and product formation of *Porphyridium purpureum*, J. Appl. Phycol. 13 (2001) 317-324.

[9] L. Trabelsi, H. Ben Houada, F. Zili, N. Mazhoud, J. Ammar, Evaluation of Arthrospira platensis extracellular polymeric substance production in photoautotrophic, heterotrophic and mixotrophic conditions, Folia Microbiol. 58 (2013) 39-45.

[10] A. Villay, Production en photobioréacteurs et caractérisation structurale d'un exopolysaccharide produit par une microalgue rouge, *Rhodella violacea* : application à

l'obtention d'actifs antiparasitaires. PhD thesis, Ecole doctorale sciences de la vie, santé, agronomie, environnement (2013) Université Blaise Pascal.

[11] A. Banerjee, R. Sharma, Y. Chisti, U.C. Banerjee, *Botryococcus braunii*: a renewable source of hydrocarbons and other chemicals. Crit. Rev. Biotechnol. 22 (2002) 245-279.

[12] A. Mishra, K. Kavita, B. Jha, Characterization of extra-cellular polymeric substances produced by micro-algae *Dunaliella salina*, Carbohydr. Polym. 83 (2011) 852-857.

[13] S. Zhang, P.H. Santschi, Application of cross-flow ultrafiltration for isolating exopolymeric substances from a marine diatom (*Amphora* sp.), Limnol. Oceanogr. Methods. 7 (2009) 419-429.

[14] H. Li, Z. Li, S. Xiong, H. Zhang, N. Li, S. Zhou, Y. Liu, Z. Huang, Pilot-scale isolation of bioactive extracellular polymeric substances from cell-free media of mass microalgal cultures using tangential-flow ultrafiltration, Process Biochem. 46 (2011) 1104-1109.

[15] V. Faerman, I. Mukmenev, I. Shreiber, Release of polysaccharide by sonication of cells (*Porphyridium* sp.), I. Acoust. Phys. 55 (2009) 270-272.

[16] E. Eteshola, M. Gottlieb, S.M. Arad, Dilute solution viscosity of red microalga exopolysaccharides, Chem. Eng. Sci. 51 (1996) 1487-1494.

[17] M.A. Guzman-Murillo, F. Ascencio, Anti-adhesive activity of sulphated exopolysaccharides of microalgae on attachment of red sore disease-associated bacteria and *Helicobacter pylori* to tissue culture cells, Lett. Appl. Microbiol. 30 (2000) 473-478.

[18] A.K. Patel, C. Laroche, A. Marcati, A.V. Ursu, S. Jubeau, L. Marchal, E. Petit, G. Djelveh, P. Michaud, Separation and fractionation of exopolysaccharides from *Porphyridium cruentum*, Bioresour. Technol. 145 (2013) 345-350.

[19] M.R. Sommerfeld, H.W. Nichols, Comparative studies in the genus *porphyridium naeg*, J. Phycol. 6 (1970) 67-78

[20] M. Gerardo, D. Oatley-Radcliffe, R. Lovitt, Integration of membrane technology in microalgae biorefineries, J. Membr. Sci. 464 (2014) 86-99.

[21] A. Marcati, A.V. Ursu, C. Laroche, N. Soanen, L. Marchal, , S. Jubeau, G. Djelveh, P. Michaud, Extraction and fractionation of polysaccharides and Bphycoerythrin from the microalga *Porphyridium cruentum* by membrane technology, Algal Res. 5 (2014) 258-263.

[22] L.O. Villacorte, Y. Ekowati, H.N. Calix-Ponce, J.C. Schippers, G. Amy, M.D. Kennedy, Improved method for measuring transparent exopolymer particles (TEP) and their precursors in fresh and saline water, Water Res. 20 (2015) 300-312.

[23] C. Denis, A. Massé, J. Fleurence, P. Jaouen, Concentration and pre-purification with ultrafiltration of a R-phycoerythrin solution extracted from macroalgae *Grateloupia turuturu* : process definition and up-scaling, Sep. Purif. Technol. 69 (2009) 37-42.

[24] M. Cheryan, Ultrafiltration Handbook. Technomic Publishing Company, Lancaster, PA. 1986, 396 p.

[25] M. Dubois, K.A. Gilles, J.K. Hamilton, P.A. Rebers, F. Smith, Colorimetric method for determination of sugars and related substances, Anal. Chem. 28 (1956) 350-356.

[26] O.H. Lowry, N.J. Rosebrough, A.L. Farr, R.J. Randall, Protein measurement with the folin phenol reagent, J. Biol. Chem. 193 (1951) 265-275.

[27] C. Hoebler, J.L. Barry, A. David, J. Delort-Laval, Rapid acid hydrolysis of plant cell wall polysaccharides and simplified quantitative determination of their neutral monosaccharides by gas-liquid chromatography, J. Agric. Food Chem. 37 (1989) 360-365.

[28] A.B. Blakeney, P.J. Harris, R.J. Henry, B.A. Stone, A simple and rapid preparation of alditol acetates for monosaccharide analysis, Carbohydr. Res. 113 (1983) 291-299.

[29] N. Blumenkrantz, G. Asboe-Hansen, New method for quantitative determination of uronic acids, Anal. Biochem. 54 (1973) 484-489.

[30] M.F. De Jesus Raposo, R.M. Santos Costa de Morais, A.M., Miranda Bernardo de Morais, Bioactivity and applications of sulphated polysaccharides from marine microalgae, Mar. Drugs. 11 (2013) 233-252.

[31] C. Safi, M. Charton, O. Pignolet, F. Silvestre, C. Vaca-Garcia, P.Y. Pontalier, Influence of microalgae cell wall characteristics on protein extractability and determination of nitrogen-to-protein conversion factors, J. Appl. Phycol. 25 (2013) 523-529.

[32] J. Heaney-Kieras, L. Roden, D.J. Chapman, The covalent linkage of protein to carbohydrate in the extracellular protein-polysaccharide from the red alga *Porphyridium cruentum*, Biochem. J. 165 (1977) 1-9.

[33] J. Heaney-Kieras, D.J. Chapman, Structural studies on the extracellular polysaccharide of the red alga, *Porphyridium cruentum,* Carbohydr. Res. 52 (1976) 169-177.

[34] E. Percival, R.A.J. Foyle, The extracellular polysaccharides of *porphyridium cruentum* and *porphyridium aerugineum,* Carbohydr. Res. 72 (1979) 165-176.

[35] S. Geresh, S.M. Arad, The extracellular polysaccharides of the red microalgae: chemistry and rheology. Bioresour.Technol. 38 (1991) 195-201.

[36] S. Geresh, N. Lupescu, S.M. Arad, Fractionation and partial characterization of the sulfated polysaccharide of *Porphyridium*, Phytochemsitry. 31 (1992) 4181-4185.

[37] S. Geresh, I. Adin, E. Yarmolinsky, Characterization of the extracellular polysaccharide of *Porphyridium* sp.: molecular weight determination and rheological properties, Carbohydr. Polym. 50 (2002) 183-189.

[38] S. Geresh, S.M. Arad, O. Levy-Ontman, R. Glaser, Isolation and characterization of poly- and oligosaccharides from the red microalga *Porphyridium sp*, Carbohydr. Res. 17 (2009) 343-349.

[39] V. Gloaguen, G. Ruiz, H. Morvan, A. Mouradi-Givernaud, E. Maes, P. Krausz, G. Strecker, The extracellular polysaccharide of *Porphyridium* sp.: an NMR study of lithium-resistant oligosaccharidic fragments, Carbohydr. Res. 339 (2004) 97-103.

[40] M. Roussel, A.vVillay, F. Delbac, P. Michaud, C. Laroche, D. Roriz, H. El Alaoui, M. Diogon, Antimicrosporidian activity of sulphated polysaccharide from algae and their potential to control honeybee nosemis, Carbohydr. Polym. 133 (2015) 213-220.

[41] B. Ismail, K.M. Nampoothiri, Molecular characterization of an exopolysaccharide from a probiotic *Lactobacillus plantarum* MTCC 9510 and its efficacy to improve the texture of starchy food, J. Food Sci. Technol. 51 (2014) 4012-4018.

[42] S.W. Kim, C. P. Xu, H. J. Hwang, J. W. Choi, C.W. Kim, J.W. Yun, Production and characterization of exopolysaccharides from an enthomopathogenic fungus *Cordyceps militaris NG3,* Biotechnol. Prog. 19 (2003) 428-435.

[43] Y.M. Lo, S.T. Yang, D.B. Min, Kinetic and feasability studies of ultrafiltration of viscous xanthan gum fermentation broth, J. Membr. Sci. 117 (1996) 237-249.

[44] W. Shu-Sen, Effect of solution viscosity on ultrafiltration flux, J. Membr. Sci. 39 (1988) 187-194.

[45] E. Eteshola, M. Karpasas, S.M. Arad, M. Gottlied, Red microalga exopolysaccharides: 2. Study of the rheology, morphology and thermal gelation of aqueous preparations, Acta Poly. 49 (1998) 549-556.

[46] Y.M. Lo, R.C. Ziegler, S. Argin-Soysal, C.H. Hsu, N.J. Wagner, Effects of intermolecular interactions and molecular orientations on the flux behavior of xanthan gum solutions during ultrafiltration, J. Food Process Eng. 32 (2009) 623-644.

[47] J. Ramus, B.E. Kenney, E.J. Shaughnessy, Drag reducing properties of microalgal exopolymers, Biotechnol. Bioeng. 33 (1989a) 550-557.

[48] J. Ramus, B.E. Kenney, Shear degradation as a probe of microalgal exopolymer structure and rheological properties, Biotechnol. Bioeng. 34 (1989b) 1203-1208.

[49] C. Harscoat, M.Y. Jaffrin, P. Paullier, B. Courtois, J. Courtois, Recovery of microbial polysaccharides from fermentation broths by microfiltration on ceramic membranes, J. Chem. Technol. Biotechnol. 74 (1999) 571-579.

[50] J. Luo, X. Hang, W. Zhai, B. Qi, W. Song, X. Chan, Y. Wan, Refining sugarcane juice by an integrated membrane process : filtration behavior of polymeric membrane at high temperature, J. Membr. Sci. 509 (2016) 105-115.

[51] M. Pritchard, J.A. Howell, R.W. Field, The ultrafiltration of viscous fluids, J. Membr. Sci. 102 (1995) 223-235.

Figure captions:

Figure 1: Evolution of permeation fluxes at various trans-membrane pressures (TMP) during the cell-free medium filtration at 1.7 $m.s^{-1}$ (×), 2.5 $m.s^{-1}$ (■), 3.3 $m.s^{-1}$ (♦), 4.2 $m.s^{-1}$ (▲) and the pure water filtration (dotted line).

Figure 2: Evolution of permeate fluxes in function of the Volume Reduction Factor (figure 2.a) or sugar concentration into the retentate (figure 2.b) during the concentration at 2.5 $m.s^{-1}$ (■), 3.3 $m.s^{-1}$ (♦), 4.2 $m.s^{-1}$ (▲) and 4 bar. Dotted lines represent the power law model, mixed lines for the gel-polarization model.

Figure 3: Evolution of the viscosity of the concentrates during the concentration stage at 3.3 $m.s^{-1}$ and 4 bar in function of the shear rate and the sugar concentrations. The consistency (K) and the behavior (n) indexes of the power law are found to be equal to 0.0009, 0.017, 0.033, 0.079 $Pa.s^n$ and 0.731, 0.653, 0.574, 0.464 for respectively the sugar concentrations of 0.48, 0.71, 1.01, 1.74 $g.L^{-1}$.

Figure 4: Evolution of the sugar retentate concentrations during the concentration stage at 2.5 $m.s^{-1}$ (■), 3.3 $m.s^{-1}$ (♦) and 4.2 $m.s^{-1}$ (▲). Dotted lines represent the trend curve (power law).

Figure 5: Abacus for the process driving of the concentration stage at 2.5 $m.s^{-1}$ (—), 3.3 $m.s^{-1}$ (····) and 4.2 $m.s^{-1}$ (----) for various filtration time, volume reduction factor (VRF) and concentration factor (CF).

Figure 6: Evolution of the permeate flux (●) and retentate conductivity (○) in the course of the diafiltration at a cross-flow velocity of 3.3 $m.s^{-1}$ and 4 bar.

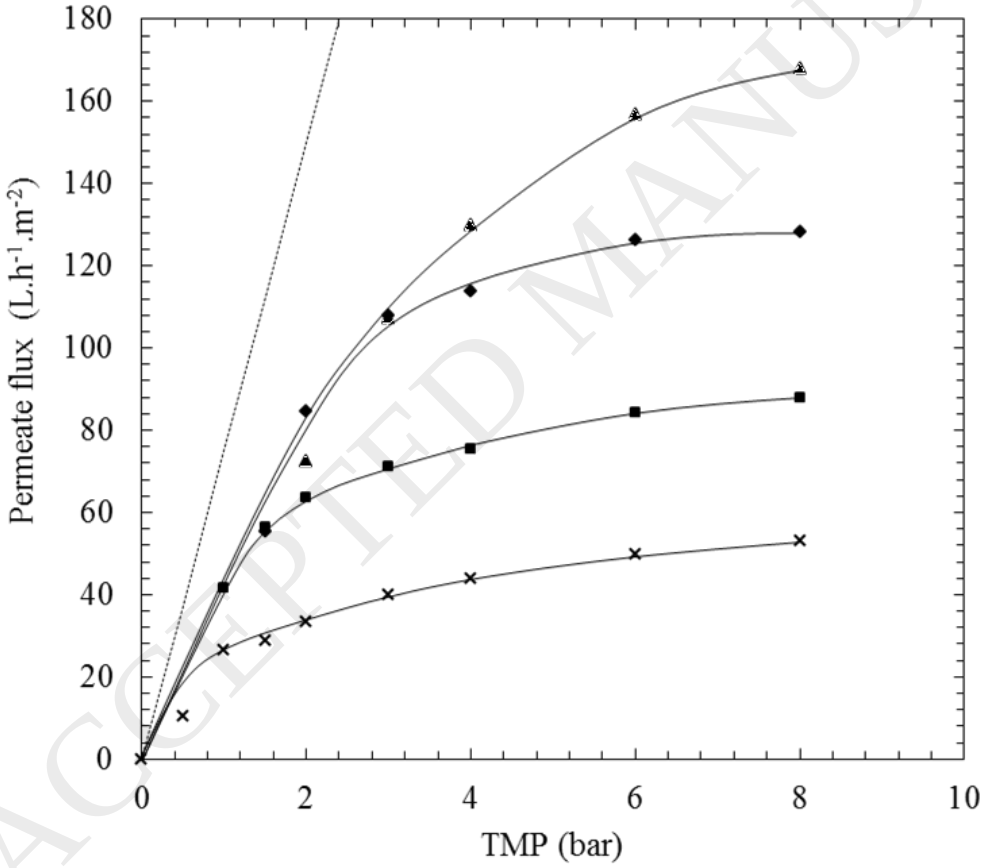

Figure 1: Evolution of permeation fluxes at various trans-membrane pressures (TMP) during the cell-free medium filtration at 1.7 $m.s^{-1}$ (×), 2.5 $m.s^{-1}$ (■), 3.3 $m.s^{-1}$ (♦), 4.2 $m.s^{-1}$ (▲) and the pure water filtration (dotted line).

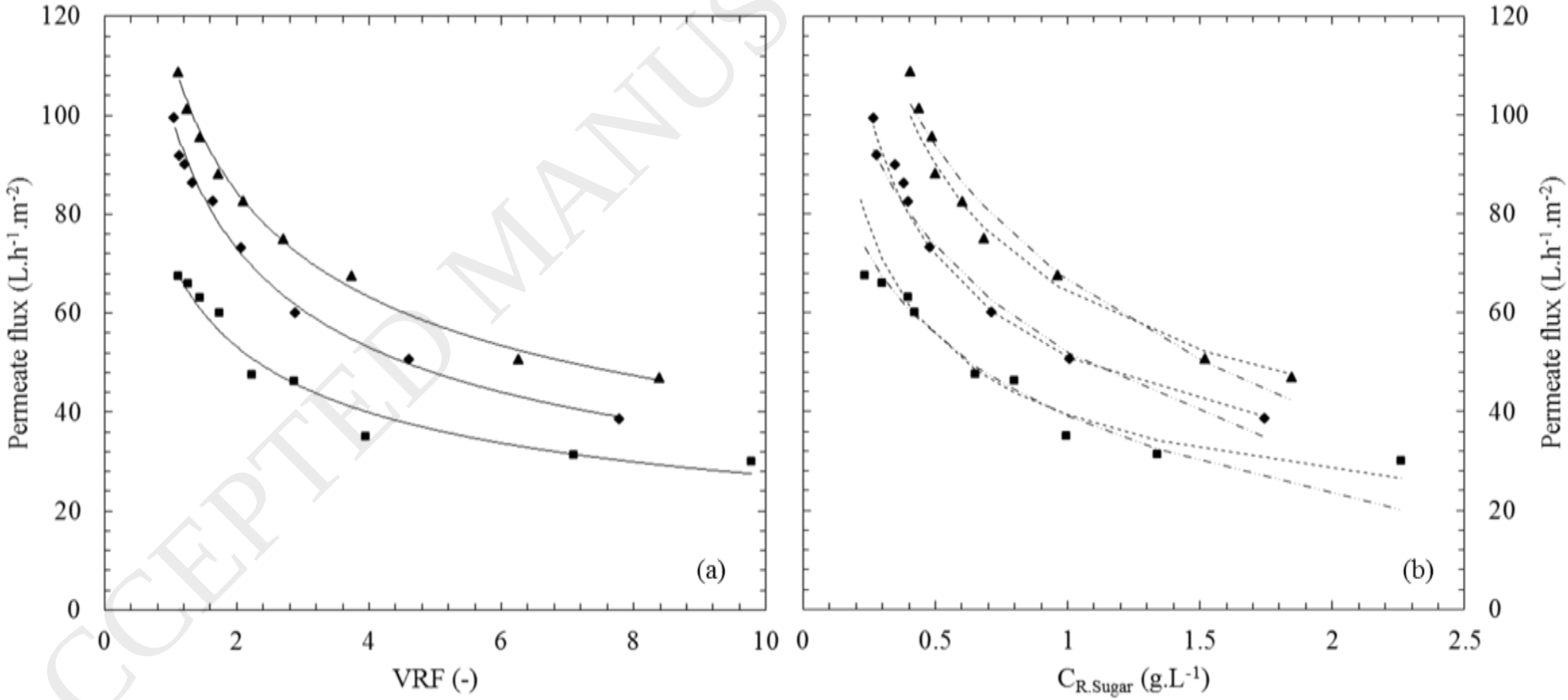

Figure 2: Evolution of permeate fluxes in function of the Volume Reduction Factor (figure 2.a) or sugar concentration into the retentate (figure 2.b) during the concentration at 2.5 m.s^{-1} (■), 3.3 m.s^{-1} (♦), 4.2 m.s^{-1} (▲) and 4 bars.Dotted lines represent the power law model, mixed lines for the gel-polarization model.

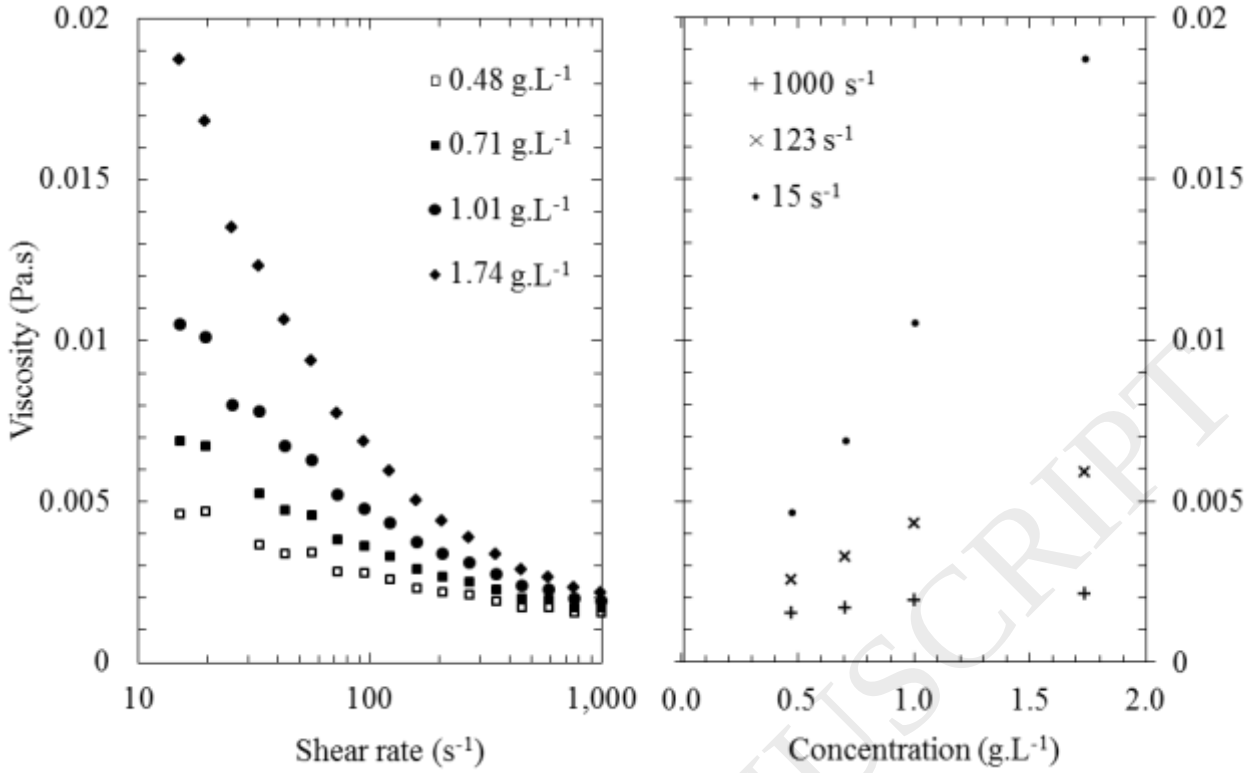

Figure 3: Evolution of the viscosity of the concentrates during the concentration stage at 3.3 $m.s^{-1}$and 4 bars in function of the shear rate and the sugar concentrations. The consistency (K) and the behavior (n) indexes of the power law are found to be equal to 0.0009, 0.017, 0.033, 0.079 $Pa.s^n$ and 0.731, 0.653, 0.574, 0.464 for respectively the sugar concentrations of 0.48, 0.71, 1.01, 1.74 $g.L^{-1}$.

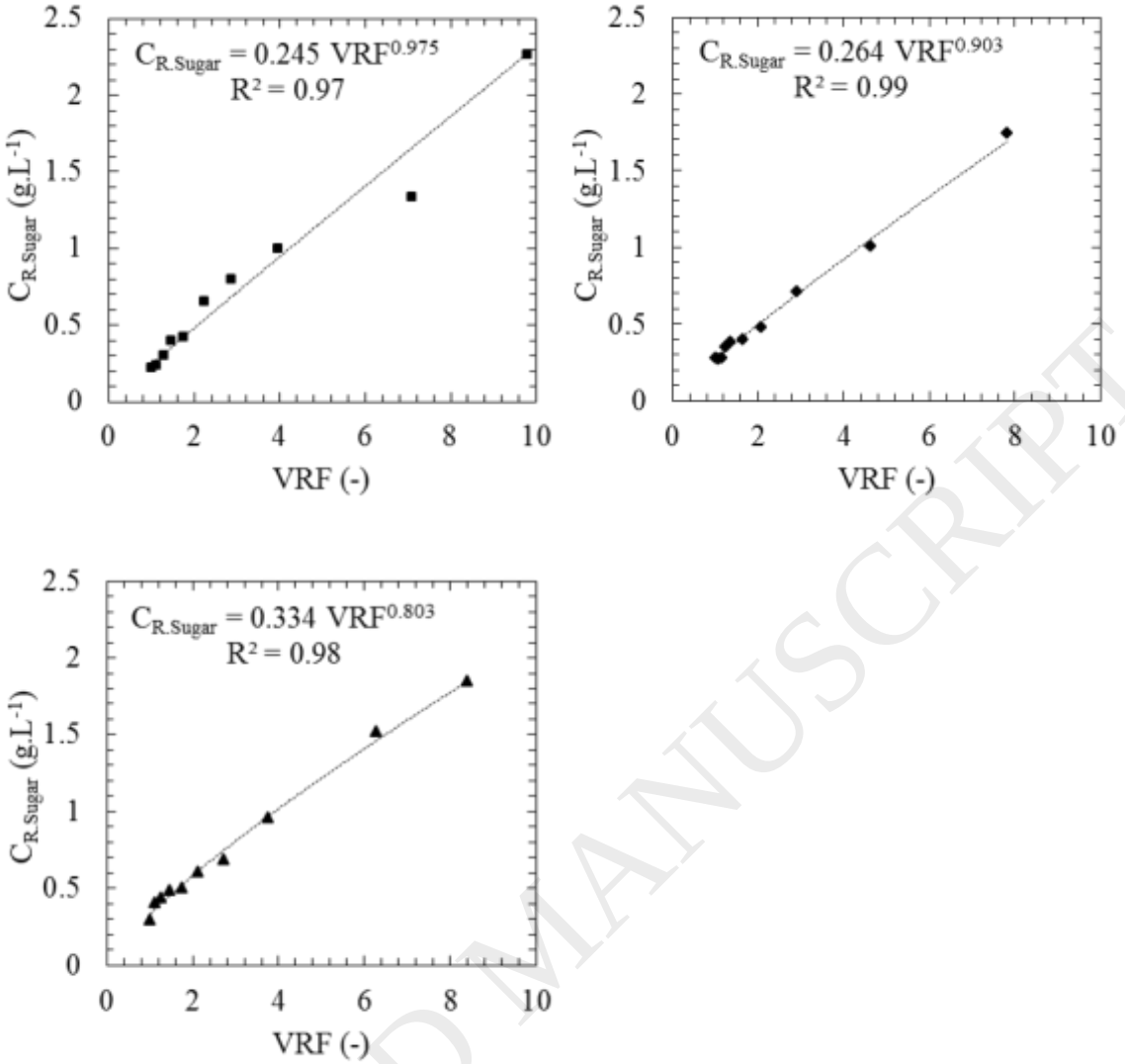

Figure 4: Evolution of the sugar retentate concentrations during the concentration stage at 2.5 m.s^{-1} (■), 3.3 m.s^{-1} (♦) and 4.2 m.s^{-1} (▲). Dotted lines represent the trend curve (power law).

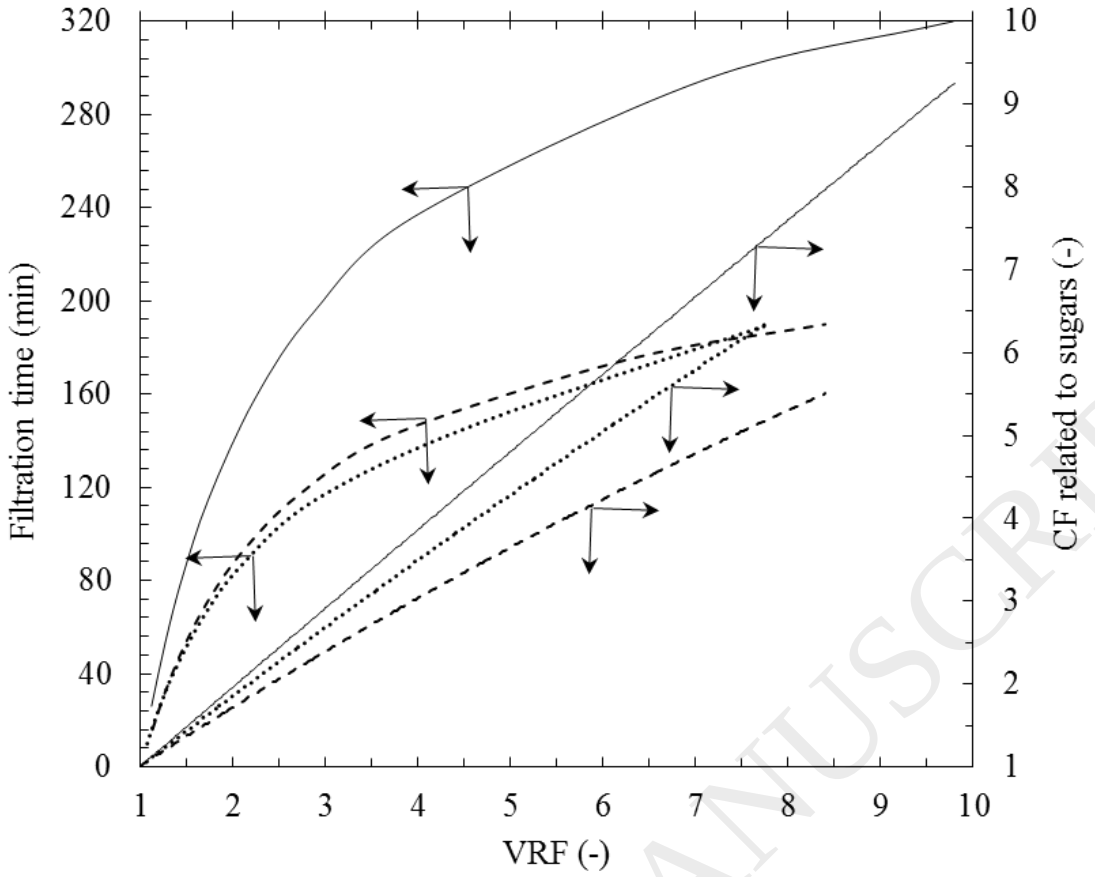

Figure 5: Abacus for the process driving of the concentration stage at 2.5 $m.s^{-1}$ (—), 3.3 $m.s^{-1}$ (····) and 4.2 $m.s^{-1}$ (----) for various filtration time, volume reduction factor (VRF) and concentration factor (CF).

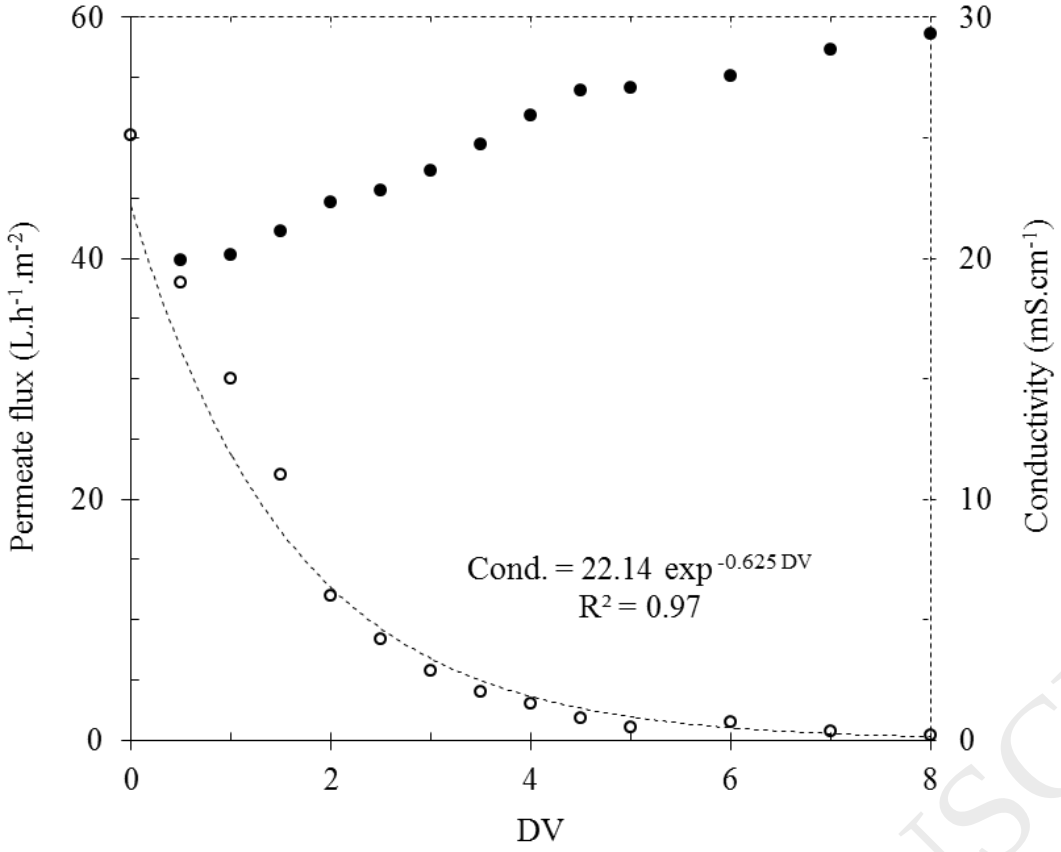

Figure 6: Evolution of the permeate flux (●) and retentate conductivity (○) in the course of the diafiltration at a cross-flow velocity of 3.3 $m.s^{-1}$ and 4 bars.

Appendice A: Method for the determination of gel-polarization model parameters

The sugar concentration profile in the vicinity of the membrane may be represented by the figure A.1.

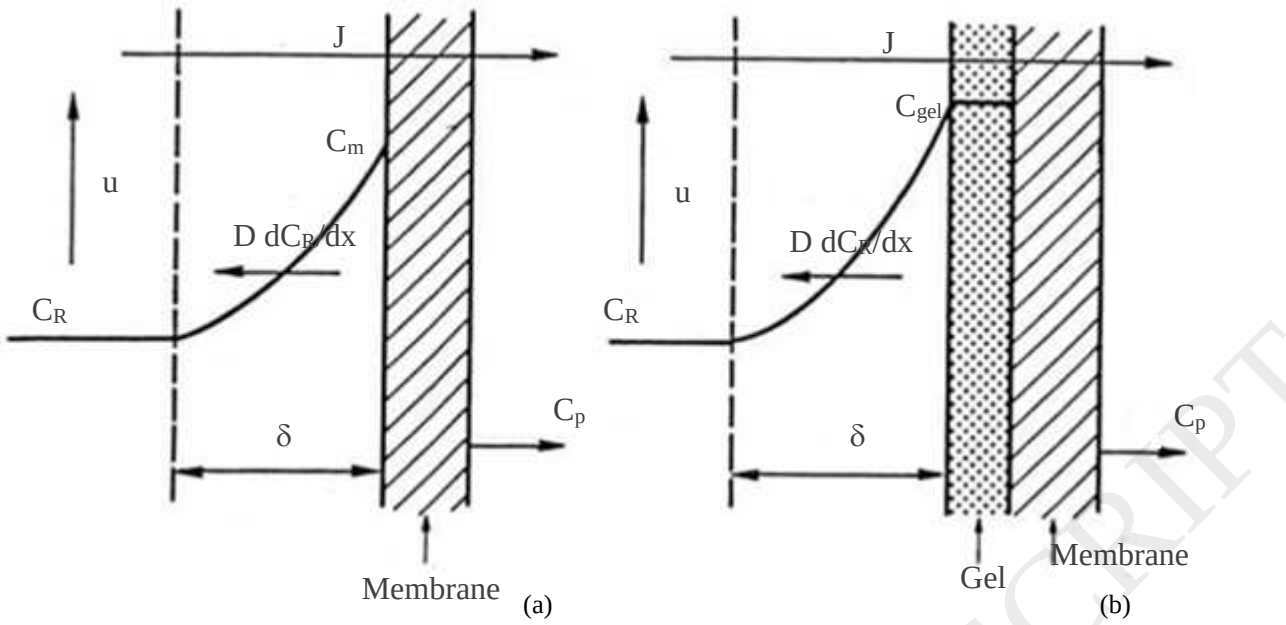

Figure A.1: Polarization concentration without (a) or with (b) gel layer at the vicinity of the membrane

The solute accumulated near the membrane surface retro-diffuses toward the solution. However, the diffusion coefficient is generally very low and the concentration C_m in the vicinity of the membrane increases with the applied pressure. It may reach the solubility limit of macromolecules and a gel may form.
In stationary operating conditions one can write:

$$J\,C_R - D\,dC_R/dx = J\,C_p$$

By considering a constant boundary layer (δ) and diffusion coefficient (D), the integration of the previous equation gives:

$$J = D/\delta \ln [(C_m - C_p) / (C_R - C_p)]$$

Where C_R, C_m, C_p represent the solute concentrations into the solution, at the membrane surface and into the permeate respectively. D/δ is the mass tranfer coefficient (k).
In the case where C_p is very low compared to C_R and a gel is built-up (C_{gel}), the permeate flux (J) is linked to the retentate concentration (C_R) during the concentration stage:

$$J = k \,.\, \ln (C_{gel} / C_R)$$

For the present work, a mean mass transfer coefficient (k) was considered during the concentration step and the sugar concentrations of the permeates were assumed negligible against retentate ones. Thus, the gel concentration can be empirically evaluated from the curve giving the permeate fluxes versus the logarithms of the sugar concentrations of retentates (Figure A.2).

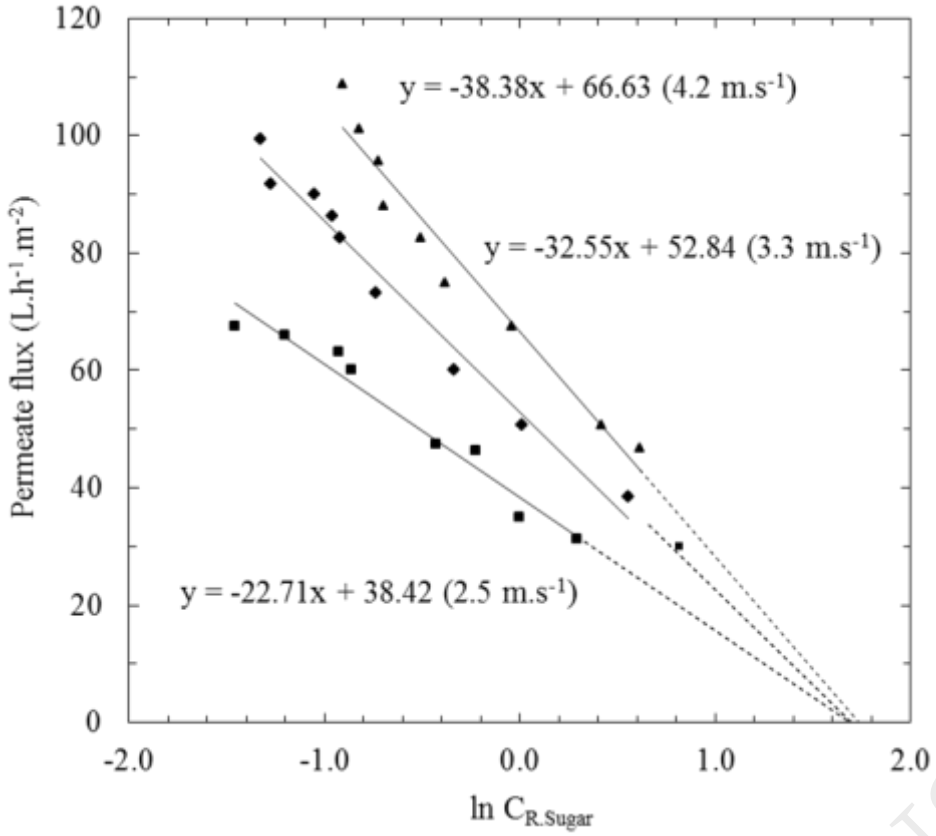

Figure A.2: Graphical representation of the permeate fluxes versus the logarithm of sugar concentration (expressed in $g.L^{-1}$) for the 2.5 $m.s^{-1}$ (■), 3.3 $m.s^{-1}$ (♦) and 4.2 $m.s^{-1}$ (▲) concentration experiments.

As a consequence, the logarithmm of the gel concentration is obtained by extending the curve to a permeate flux equal to zero. The mass transfer coefficient is the slope of the regression line.

Table captions:

Table 1: Material balance of the concentration and diafiltration stages

Table 2: Mass average molar mass (M_w), Number average molar mass (M_n), Polydispersity index (I_p), Gyration radius (R_g) of the feedstock, final retentate of the concentration experiment at 2.5 $m.s^{-1}$, 3.3 $m.s^{-1}$ and 4.2 $m.s^{-1}$.

Table 3: Monosaccharide contents of dry matter (% - w/w) into various samples

Table 1: Material balance of the concentration and diafiltration stages

		CONCENTRATION at 2.5 m.s^{-1}		CONCENTRATION at 3.3 m.s^{-1}		CONCENTRATION at 4.2 m.s^{-1}		DIAFILTRATION at 3.3 m.s^{-1}		OVER ALL
	Duration (min)	320		190		190		195		385
	VRF or DV (-)	9.8		7.8		8.4		8		-
	CF (-)	10.4		6.4		6.3		1.0		6.4
	J_{mean} (L.h^{-1}.m^{-2})	49.8		68.9		81.2		49.7		-
Concentrations (g.L^{-1}) and recovery rates (%)										
	Feed	Final retentate		Final retentate		Final retentate		Final retentate		
	C (g.L^{-1})	C (g.L^{-1})	Y_R (%)	C (g.L^{-1})	Y_R (%)	C (g.L^{-1})	Y_R (%)	C (g.L^{-1})	Y_R (%)	Y_R (%)
Sugar	0.22/0.27/0.29*	2.26	106.3	1.74	82.9	1.85	74.9	1.74	100.0	82.9
Protein	0.03	0.18	59.9	0.15	62.6	0.17	63.9	0.12	81.5	51.0
Dry matter	16.4	20.6	12.8	20.2	15.9	18.8	13.7	ND	-	-
Ash	15.2	16.6	11.2	16.7	14.1	15.8	12.4	ND	-	-

*Each value corresponds respectively to the concentration experiment at 2.5, 3.3 and 4.2 m.s^{-1}; Y_R : recovery rate into the retentate calculated from the final and initial concentrations and volumes; DV: final number of diavolumes(V_w/V_0); VRF: final volume reduction factor; CF: final concentration factor (calculated on sugars). ND: not determined

Table 2: Mass average molar mass (M_w), Number average molar mass (M_n), Polydispersity index(I_p), Gyration radius (R_g)of the feedstock, final retentate of the concentrationexperiment at 2.5 $m.s^{-1}$, 3.3 $m.s^{-1}$ and 4.2 $m.s^{-1}$.

Sample	M_w (Da)	M_n (Da)	I_p (-)	R_g (nm)
Feedstock	$2.4x10^6$	$2.0x10^6$	1.18	173
Concentration at (2.5 $m.s^{-1}$)	$1.8x10^6$	$1.6x10^6$	1.13	148
Concentration at (3.3 $m.s^{-1}$)	$2.1x10^6$	$1.8x10^6$	1.13	167
Concentration at (4.2 $m.s^{-1}$)	$2.2x10^6$	$2.0x10^6$	1.11	169

Table 3: Monosaccharide contents of dry matter (% - w/w) into various samples

Monosaccharides	Feedstock	Final retentate of the **concentration** at			Final retentateof the **diafiltration**at 3.3 $m.s^{-1}$
		2.5 $m.s^{-1}$	3.3 $m.s^{-1}$	4.2 $m.s^{-1}$	
Xylose	0.2	2.2	1.6	1.9	15.5
Galactose	0.2	2.2	1.7	2.0	16.3
Glucose	0.1	1.0	0.6	0.9	6.7
Glucuronic acid	0.1	2.3	1.5	1.0	10.4
Sum	0.6	7.7	5.4	5.8	48.9